EFFECT OF SHEAR ON THE RHEOLOGY AND CRYSTALLISATION OF PALM OIL

E. TARABUKINA [1,3], F. JEGO [2,4], J.-M. HAUDIN [1], P. NAVARD [1] and E. PEUVREL-DISDIER [1]

[1] MINES ParisTech, CEMEF - Centre de Mise en Forme des Matériaux, CNRS UMR 7635, BP 207, 1 rue Claude Daunesse, 06904 Sophia Antipolis Cedex, France

[2] Thermofisher Scientific, 16 avenue du Quebec, Silic 765, 91963 Courtaboeuf Cedex, France

[3] Permanent address: Institute of Macromolecular Compounds, Russian Academy of Sciences, Bolshoy pr. 31, 199004 St.-Petersburg, Russia

Corresponding author: E. PEUVREL-DISDIER
Tél: +33-(0)4-93-95-75-89
Fax: +33-(0)4-92-38-97-52
E-mail: edith.disdier@mines-paristech.fr

Short version of title: Crystallisation of palm oil under shear

Choice of journal section where article should appear

Concise Reviews and Hypotheses in Food Science
Food Chemistry
Food Engineering and Physical Properties
Food Microbiology and Safety
Sensory and Food Quality
Nanoscale Food Science, Engineering, and Technology
Health, Nutrition, and Food
Toxicology and Chemical Food Safety

Previous address(es)
[4] Malvern Instruments Ltd, Enigma Business Park, Grovewood Road, Malvern, Worcestershire, UK. WR14 1XZ, U.K.

ABSTRACT:

This paper reports on the impact of shear on crystallisation upon cooling of palm oil. Samples were cooled down under shear from 70 °C to 10 °C, then kept at this temperature, while performing rheological measurements using a controlled shear rate rheometer and rheo-optical observations using optical microscopy and small-angle light scattering. Shear rates between 1 and 300 s^{-1} were investigated. Two crystallisation steps were observed, characterized by associated viscosity increases. The effect of shear on these two crystallisation processes was investigated. Shear was shown to influence almost all the steps of the structuring process of the crystallizing palm oil. The spherulite size and growth rate during the first crystallisation are affected by shear. The onset time of the secondary crystallisation process strongly depends on the extent of shear. The steady state structures after the first and the secondary crystallisation processes constituted of a suspension of aggregates of spherulites are controlled by the applied shear rate.

PRACTICAL APPLICATION:

The texture of crystallised vegetal fats and subsequent end product properties depend on the structure developed during the crystallisation process. This structuring process is strongly influenced by the thermo-mechanical history submitted to the product (cooling rate, degree of undercooling, annealing time, application of flow). This paper shows how the extent of shear affects the different steps of the crystallisation and aggregation processes in the case of palm oil after the first crystallisation.

KEY WORDS:

Palm oil, crystallization, shear, rheology

Introduction

Vegetal fats are commonly used in food industry, such as in dough and biscuit fillings. These materials are mainly constituted of different families of triglycerides which crystallise at different temperatures depending on their chemical composition. Many studies concerned the compositional effect of triglycerides on the crystal types and crystallisation process ((Jacobsberg and Ho, 1976), (Berger and Wright, 1976), (Persmark et al., 1976), (Kawamura, 1979), (Timms, 1984), (Siew and Ng, 1995 and 1996), (Walstra et al., 2001)). Different polymorphisms exist. The general scenario for fat crystallisation is first nucleation and growth of crystals, followed by their aggregation due Van der Waals attraction ending up with the formation of a crystalline 3D-network (Walstra et al., 2001).

Palm oil is mainly composed of three types of triglycerides, trisaturated (mainly PPP that is tripalmitin), disaturated (mainly POP that is 2-oleodipalmitin) and monosaturated (mainly POO that is 1-palmitoyl-2-3-dioleoylglycerol). The melting behaviour of this blend is characterised in differential scanning calorimetry by two endotherms in the temperature range of -23 °C and 43 °C ((Ng and Oh , 1994), (Siew and Ng, 1999)). The high melting temperature mainly involves the fully saturated triglycerides (trisaturated) whereas the lower melting one mainly involves the monosaturated ones. At room temperature, palm oil is a semi-solid material which texture, hardness and spreadability depend on the amount, size and tri-dimensional organisation of the crystals (fat crystal network) in it.

During industrial processes, the thermomechanical history may affect both the nature of the species which will crystallise and the tri-dimensional organisation of the crystals. Crystallisation may occur at rest, such as in a cooling tunnel, or instead occur under conditions of high shear and large temperature gradients, such as in a scraped surface heat exchanger. For this reason, several studies were recently devoted to the better understanding of fat crystallisation including palm oil under different thermo-mechanical conditions.

The crystallisation of fat results in the creation of a fat crystal network but involves different steps with classical crystal nucleation and growth, but also polymorphism transitions, aggregation due to Van der Waals attraction which continues until a 3D-network is formed (Walstra et al., 2001). Due to this multi-step crystallisation process, the effect of shear can be multiple (see for example the introduction part of (Kloek et al., 2005) or (De Graef et al., 2008)). Shear can affect:

- nucleation, orientation of crystallites, crystal structure and size, polymorphism transition and orientation of primary crystals ,
- aggregation of the crystals. Shear can promote aggregation. If the shear is further increased, shear can induce the aggregate break-up. But shear can also induce internal rearrangements of the aggregates, leading to more compact assemblies,
- the fat crystal network via fragmentation of the network, rearrangement of the fragments.

Different techniques can be used to gain information on the crystallisation process under shear:

- rheo X-ray (shear coupled with X-ray diffraction) allows the characterisation of crystallites, polymorphism type and transition and crystal orientation (Mazzanti et al. 2005, 2007),
- rheo-pNMR (pulsed NMR) can be used to determine the solid fat content (fraction of crystallised fat) (Mazzanti et al., 2008),
- rheo-optics (polarized optical microscopy) allows the direct observation of the crystal growth and the aggregation process (De Graef et al., 2008),
- rheology is also a very interesting technique:
    - the large increase of solid fat content during crystallisation and aggregation process results in a large viscosity increase,
    - the measurement of storage and loss moduli and phase angle enables to evaluate the aggregation, network formation and post-hardening processes (De Graef et al, 2006).

Recent studies were conducted on palm oil crystallisation under shear at different isothermal conditions 17, 18 and 22 °C ((Mazzanti et al., 2005), (De Graef et al., 2008)). These conditions were chosen since they gave rise to the crystallisation of different fractions of palm oil (crystallisation of high melting fraction at 22 °C and of high and medium melting fractions at 17-18 °C). Crystallisation proceeded through α nucleation and successive α→β' polymorphic transformation. Shear had no effect on the onset of α crystallisation but accelerated the polymorphic transition.

As mentioned, previous studies focussed on the effect of shear on the crystallisation of partial fractions of palm oil. In the present work, we investigated the effect of shear on

the full fraction resulting from the first crystallisation of palm oil. Therefore, the isothermal condition was fixed at 10 °C. This means that when the isotherm condition was reached, the first crystallisation was close to total. The fact to work at a lower temperature relative to previous works implied crystallisation of larger solid fat contents. The impact of shear on the structural organisation of this larger crystallised product is addressed in this paper. The crystallisation process was followed during shear in the defined thermal conditions using rheometry (viscosity), optical microscopy and small-angle light scattering.

Materials and Methods

Palm oil

The sample used was a commercial refined palm oil kindly provided by Danone. The composition was 50% of saturated fatty acids, 40% of mono-unsaturated and 10% of poly-unsaturated fatty acids. The iodine value was 50 g of iodine per 100g. Palm oil was used as received.

Differential Scanning Calorimetry (DSC)

DSC experiments were performed with a DSC-7 calorimeter (from Perkin Elmer, Masachussets, USA) using aluminium pans.

Shear rheology

A Bohlin controlled strain rheometer (from Malvern, Worcestershire, UK) equipped with different geometries was used (two parallel plate geometries d = 60 mm or 40 mm, cone-

and-plate 4°/40 mm). All surfaces of the different shear geometries were smooth. The cooling of the Bolhin rheometer was ensured via a Peltier plate (under the base plate). The Peltier plate was chosen in order to ensure a good and reproducible control of the temperature along the cooling step and a direct transition to the isothermal temperature (no overshoot). The temperature control being ensured by the bottom plate, the gap was fixed to a low value (0.3 mm). This value was chosen after different viscosity measurements during crystallisation at different gap values. A measurement at 1 mm gap showed an effect of the temperature gradient for this large gap resulting in a lower viscosity. Gap values between 0.3 and 0.5 mm gave similar steady state viscosities.
Crystallisation being controlled by the temperature condition, it was decided to perform all measurements at a cooling rate of –5 °C/min in order to compare measurements performed in well defined thermal conditions.

The three shear geometries had advantages and drawbacks:

- the cone-and-plate geometry presents the advantage of a constant shear rate. However with the 4°/40 mm geometry, the gap at the edge of the plate was 1.4 mm wide. Following the gap tests with the parallel plate geometry, a temperature gradient existed between the bottom plate and cone at large gaps (close to the outside of the sample),
- the parallel plate geometry has the drawback of a linear shear rate variation between the centre of the plate and the edge. The low value gap ensured a good temperature control. A 60 mm diameter plate was used in order to have a larger torque in the molten state and thus a better accuracy of the viscosity in this zone.

However the use of the 60 mm plate-and-plate geometry gave less reproducible results. The setting of the sample (filling of the gap) was more delicate than for the 40 mm plate and a small difference in the volume sample resulted in a small shift in the viscosity curve.

Measurements were reproducible despite small deviations were sometimes noted in the zone A of the viscosity part (defined in Figure 5). For example all viscosity curves should superimpose in zone A where palm oil is in the molten state. However, this is not what is observed on Figure 5 for the shear rate of 100 s^{-1}. Although a similar shift was also measured by De Graef et al. (2008) for the same shear rate in the same temperature range (Figure 6 of their paper), the fact that we did not observe this deviation with the other geometries and at higher shear rates let us think that this was due to an experimental artefact. Small viscosity deviations in zone A of the viscosity curves were noted in the 60 mm parallel plate geometry (see Figure 10). As mentioned in the previous paragraph, this was attributed to the non correct filling of the sample in this geometry.

Rheo-optical techniques

Rheo-optical shear experiments were conducted in a high-temperature transparent parallel disk shearing device (manufactured by Linkam Scientific, Epsom, Surrey, UK). The sample is placed between two circular quartz windows, which are in close thermal contact with a silver block heater. The shear cell was mounted on an optical microscope equipped with a CCD camera. A 0.3 mm gap was used for optical microscopy observations.

The same transparent shearing device was used to perform small-angle light scattering (SALS) experiments. A 0.2 mm gap was used in this case in order to minimize multiple scattering. The experiments were conducted using a 633 nm wavelength laser passing through the windows of the shear cell. The scattering pattern was formed on a paper screen and recorded by transparency by a black and white video camera. The pattern was recorded in HV mode (between crossed polarisers). When a four-lobe pattern was observed (characteristic of a spherulitic organisation (Haudin and Navard., 1990)), the location of the maximum of intensity (expressed via the scattering vector) was determined from the intensity profile using a custom-made image analysis software dedicated to analyse scattering patterns. The size of the spherulite (R) was calculated using the Rayleigh-Gans-Debye relationship:

$$q_{\max} R = 4.1 \text{ for a spherulitic entity}$$

where $q_{\max}$ is the scattering vector at the maximum of intensity of the lobs, $q = \frac{4\pi}{\lambda}\sin\left(\frac{\theta}{2}\right)$ with λ the wavelength of the laser and θ the polar angle.

Results and Discussion

CRYSTALLISATION AT REST

DSC experiments

An example of a palm oil cooling thermogram is shown in Figure 1 for different cooling rates, showing the two crystallisation peaks. The first crystallisation peak was observed between 15 and 20 °C depending on the cooling rate and that the second crystallisation

peak was around 0 °C (see Figure 1). At -5 °C/min, cooling rate chosen in our experiments, the first crystallisation started around 22 °C and ended around 3 °C with its maximum peak at 18 °C. This cooling thermogram is classical for palm oil and similar to the one measured by Ng and Oh (1994).

A DSC experiment was also performed in identical thermal conditions as for the rheological measurements. The palm oil sample was cooled down from 70 to 10 °C with cooling rate of –5 °C/min and then held at 10 °C. The heat flow variation was recorded in the isothermal mode at 10 °C and is shown in Figure 2. It shows that, after the first crystallisation starting at 22 °C (as observed in Figure 1), a gradual exothermal process took place starting after 3-4 minutes (time 0 = onset of isotherm) and maximum at around 15 minutes, showing the presence of a secondary crystallisation. The height of the peak of this exotherm was much smaller than the first crystallisation peak (when compared with the same unity mW/°C). The presence of an exothermal peak during an isotherm at 10 °C was also reported by Ng and Oh (1994). With their sample, they found two exothermal peaks, one immediately at the onset of the isotherm and a very broad peak starting after 15 minutes. This first peak could not be detected in our measurements due to an experimental artefact. A short time was lost between the end of the cooling ramp and the starting of the isothermal one since the apparatus did not allow us to run successive experiments without modifying the experimental set-up parameters in between. The authors also determined the solid fat content during the isotherm by pulsed-NMR. The two step crystallisation was also shown by the evolution of the solid fat content during isotherm. At 9 °C, a rapid increase of solid fat content at time 0 was first

recorded levelling at 17% after a few minutes followed by a second increase of solid fat content starting 15 minutes after the isotherm onset, approaching a steady state value of 48 % of solid fat content after 80 minutes. This tends to show that an additional crystallisation is occurring during the isothermal step after the first crystallisation (during the cooling ramp).

Optical microscopy and SALS observations:

The crystallisation of palm in absence of shear is illustrated in Figure 3 (pictures referred to 0 s^{-1}). At 22 °C, crystals, seen as rod-like crystals, appeared. These crystals are composed of nanoscopic crystallites which cannot be observed by optical microscopy. Next, spherulitic entities (consisting of numerous needles) were observed (Figure 3, 20 and 19.4 °C, picture enlarged in Figure 4.a). The number of spherulites increased and aggregates were formed in time (Figure 3, 19.4 and 18.7 °C). At 17 °C, all the space looked like being full of crystalline entities, as seen by transmission optical microscopy. At this temperature, only a small fraction of palm oil was crystallised (according to the DSC, Figure 1). However a suspension with a few percent solid volume fraction can be sufficient to give the impression in optical microscopy of volume filling if the gap is large enough, which is the case here. These features are classical for the crystallisation of vegetable fats and palm oil ((Van Putte and Bakker, 1987), (Mazzanti et al., 2005), (De Graef et al., 2008)). The exact polymorphism of the crystals was not determined in this study but different authors identified an α nucleation followed by an $\alpha \rightarrow \beta$' phase transition in isothermal conditions ((Persmark et al., 1976), (Mazzanti et al., 2005) and (De Graef et al., 2008)).

The spherulitic organisation of crystals was confirmed by SALS where a classical four lobe-pattern (lobes oriented at 45° relative to the polarizers) was obtained between crossed polarizers (Figure 4-b).

CRYSTALLISATION OF PALM OIL UNDER SHEAR

Thermomechanical history

Based on calorimetry measurements and in order to focus on the first crystallisation, it was decided to apply a constant shear rate during the cooling stage and to stop this cooling at 10 °C, temperature at which the first crystallisation was almost finished and the second crystallisation was not started (Figure 1).

The following thermomechanical history was thus applied to all samples:

- thermostabilisation at 70 °C for 15 min without shear in order to erase previous thermo-mechanical history,
- cooling from 70 °C to 10 °C at a constant cooling rate -5 °C/min,
- holding at 10 °C for 15 min,
- under flow, a constant shear rate was applied during the cooling and isothermal steps.

Viscosity evolution during cooling

The general evolution of the viscosity of palm oil when cooling from 70 °C down to 10 °C and then keeping this temperature constant is given in Figure 5 at -5 °C/min cooling rate for different shear rates with the cone-and-plate geometry.

Figure 5 shows a succession of viscosity changes which correspond to physical modifications occurring in the palm oil during cooling. In order to describe these different states, viscosity curves were divided into six zones:

Zone A: The viscosity was increasing with time when the sample was cooled down from 70 °C to about 20 °C. Palm oil was molten in this temperature range. The viscosity increase was only due to the temperature decrease.

Zone B: Around 20 °C (600 s), a viscosity jump occurred. It was the signature of the onset of palm oil crystallisation as seen by DSC.

Zone C: Between 700 s and 900 s, the viscosity was constant. This corresponded to the onset of the isothermal zone where the sample was sheared at a constant temperature of 10 °C. Palm oil was in a state where the first crystallisation was finished. A steady state was reached.

Zone D: After a certain time where the viscosity was constant (zone C), the viscosity increased again. This was more marked at low shear rates. The end of this zone showed a second plateau.

Zone E: Second viscosity plateau.

Zone F: The viscosity started to strongly oscillate, mainly at low shear rates.

Viscosity curves are correlated to structure evolution. Figure 3 shows different states of crystallisation for the different shear rates as observed by optical microscopy. The first steps of crystallisation were very similar than the ones describes at rest. A particular

attention was paid to what happened under shear at low shear rate (Figure 3, 10 s^{-1}) in order to have a good description of the different steps:

1. first crystals and spherulites were formed, their number and size increased. Crystals were moving as individual bodies,
2. spherulites started to meet because of the increase of crystalline fraction. They formed aggregates composed of a few spherulites. Due to their particular shape, they had a different motion relative to isolated spherulites and thus could well be distinguished,
3. further increasing the crystalline fraction: these aggregates grew in size. These larger entities had a slower motion due a collaborative motion,
4. around 890 s, the sample was moving as a single body. All the aggregates were connected together and formed a rigid network,
5. if the shear was continued to be applied, local breakages of the fat network were observed. This destruction of the network was observed around 1000 s. After the network destruction, the motion of large fragments in suspension in a clear liquid phase could be observed. Figure 4.c shows a picture of the crystalline entities suspended in the segregated interstitial liquid. The entities were large, nearly spherical and compact relative to the initial spherulites with no trace, at this stage, of the primary rod-like crystals. Aggregates of a few spherulites were also present.

The crystallization under shear at 100 s^{-1} (Figure 3) showed similar features at the beginning with the appearance of first crystals , formation of spherulites, aggregates of spherulites, increase of the crystallized volume fraction and the packing density.

However, the motion of the complete sample as a single solid body was never observed. In these two cases, the shear resulted in the motion of a multitude of individual entities. The size and shape of the entities could not be clearly distinguished due to the large crystalline volume fraction.

The first viscosity jump corresponds to the beginning of crystallisation of palm oil, with the formation of rod-like crystals followed by the appearance of spherulites and subsequent aggregation. A steady state (first viscosity plateau) was reached during the isothermal condition. The first viscosity plateau corresponded to the flow of a suspension of aggregates of spherulites in the molten phase where the motion of isolated aggregates could be observed. The first viscosity jump and subsequent steady state were also reported by De Graef et al. (2008) in experiments conducted at 18 °C. After some time, a second viscosity increase was observed. The motion of larger entities at larger scales was associated with the second viscosity jump. For large shear rates, a steady state (second viscosity plateau) was reached. For low shear rates, no steady state could be attained. The networking of the system went on up to the state where the sample moved as a solid body, either moving as a whole or fully stopped (indicating slippage of the sample at one of the glass plates). Further application of shear led to the break-up of the network and the appearance of segregation with a fully aggregated phase and a liquid one. This last step lead to the appearance of oscillations of the viscosity at low shear rates.

The different zones are examined in more details in the following.

Zone A: Viscous flow of molten palm oil

In this zone, palm oil is in the molten state, which is characterised by a Newtonian behaviour. Between 70 and 25 °C, the viscosity varies with the temperature according to the Arrhenius law:

$$\eta = \eta_o \cdot e^{\frac{\Delta E_a}{kT}}$$

η being the viscosity of the oil at a given temperature T, E_a being the activation energy, k being the Boltzman constant, and η_0 being a constant. An activation energy equal to 5.1×10^{-20} J/mole was calculated for palm oil when submitted to a cooling rate of -5 °C/min. This value is in the range of activation energies for low molecular weight Newtonian liquids (e.g. $E_a=8.3\times10^{-20}$ J/mole for glycerine (Grigoriev et al., 1997)).

Zone B: First viscosity jump

Effect of shear on the first crystallisation temperature

The first sharp increase of the viscosity is related to the crystallisation (crystallisation and aggregation) of palm oil. This corresponds to the first crystallisation seen by DSC. The start of the viscosity jump, corresponding to a given temperature T_c during the cooling step, is an indicator of the onset of crystallisation. The variation of this crystallisation temperature versus the applied shear rate is reported in Figure 6 for the different shear geometries and techniques. The temperatures of appearance of first crystals (rod-like) and spherulites as seen by optical microscopy and S.A.L.S. (temperature of first observation of the four-lobe pattern) are also indicated.

The comparison of results obtained by different techniques, different temperature control systems, gradients, mass transfers, static relative to dynamic experiments and different shear geometries, is always a delicate exercise. The first observation is that there is a good agreement between the crystallisation temperatures corresponding to the beginning of the crystallisation peak (as measured by DSC) and the formation of first crystals (rod-like crystals, observed by optical microscopy). The appearance of spherulites observed by optical microscopy or S.A.L.S happened at slightly lower temperatures and was more easily detected by S.A.L.S. The detection of crystallisation via the onset of viscosity jump gave more scattering in the data. No clear evidence of a potential effect of the shear rate on the onset of crystallisation could be deduced from the measurements. A slight variation of the crystallisation temperature with the shear rate could be deduced from the measurements in cone-and-plate geometry where the shear rate was constant: first increase of crystallisation temperature with shear rate and then decrease. However, these tendencies were not supported by local observations in the Linkam cell (parallel plates) either by optical microscopy (Figure 3) or light scattering (Figure 7), with the restriction that these local observations were performed in a parallel plate geometry.

Mazzanti et al. (2005) and De Graef et al. (2008) showed that crystallisation of palm oil in isotherm conditions (17-18, 22°C) happened via an α nucleation followed by a $\alpha \rightarrow \beta'$ polymorphic transition. They showed that whereas the α nucleation temperature did not depend on the applied shear rate, the $\alpha \rightarrow \beta'$ transition was accelerated by the shear rate. The two-step crystallisation process was also evidenced by a two-step continuous viscosity increase (seen by two different slopes). Our measurements did show a single

step viscosity jump with no effect of the applied shear rate. It is not possible to assert from our measurements that the two step crystallisation process did not occur. If the α nucleation was immediately followed by the α→β' transition, the effect of shear rate on the α→β' transition would be limited by the α nucleation process. The two-step 7 crystallisation process would be seen as a single step with no dependence on shear.

Size evolution during this step:

S.A.L.S. enabled us to follow the variation of the spherulite size versus time at different shear rates. S.A.L.S. gives access to an averaged size with an enhanced weight on large 2 entities. The scattering patterns and corresponding spherulite sizes versus the applied shear rate and temperature are reported in Figure 9.

The SALS patterns (Figure 7.a) illustrate that while the crystallisation proceeded, a four-lobe pattern appeared and could be followed for some time before giving rise to a different pattern. Multiple scattering and pattern modification after the spherulitic step 7 (aggregation and possible structural rearrangements) limited the range of use of S.AL.S. to follow the crystalline entity size over the whole process. The crystalline entity size could only be determined when the pattern was a four-lobe pattern.

The observation of the patterns at the different shear rates shows that there was a difference in spherulite size at the same temperature. Larger scattering entities give rise to scattering patterns at smaller angles. The size difference is confirmed by the size evolution shown in Figure 7.b. The larger the shear rate was, the larger the spherulites were at a given temperature and the earlier they were detected since the scattering intensity is proportional to the square of the size. For example around 21 °C, the

spherulites in palm at rest or under a small shear rate should have a mean radius around 5 μm (extrapolation from the growth rate measured), in comparison with 9 μm at 10 s^{-1} and 18 μm at 100 s^{-1}. The difference in size is also clearly seen on optical microscopy observations (Figure 3, comparison of pictures around 20 °C for 0, 10 and 100 s^{-1}).

The growth rates calculated from the size evolution measured by S.A.L.S. are reported in Table 1. Results did not show a large variation in the growth rate between static and low shear conditions. But the crystallisation rate at 100 s^{-1} was much faster. It is four times faster at the beginning and then seems to slow down. Very few data exist in the literature on the crystal growth rate of palm oil. Spherulite growth rates lower than 1 μm/min or around 2 to 3 μm/min were measured on different palm oil compositions in static conditions (respectively by Kawamura (1979) and Van Putte and Bakker (1987)). After a linear growth rate of the crystal size, Kawamura (1979) also observed a levelling of the crystal size. Spherulite diameters between 10 and 60 μm were determined. The growth rates measured in static conditions are thus in the same range.

Optical microscopy and light scattering observations showed that although the effect of l shear on the onset of crystallisation was not obvious, there was a clear effect of the applied shear rate on the spherulite size and growth rate.

Hydrodynamic effect on the structure evolution:

The formation and growth of individual crystals cannot explain the large viscosity increase. The crystallisation process with its characteristic parameters like, nucleation speed, crystal size and growth rate, and the almost concomitant aggregation process versus applied shear rate should be considered when trying to predict the viscosity jump.

Aggregation mainly contributes to the large viscosity increase since the volume of an aggregate is larger than the volume fraction of individual entities with the entrapped liquid. The effect of shear on the crystal size and growth rate was reported in the previous paragraph. Its effect on aggregation can be due to several factors (see for example (Zhou et al., 1995), (Kloek et al. (2005) for fat)). Shear promotes aggregation via collision (collision frequency proportional to shear rate). However this effect is limited by the time needed for an effective aggregation to take place. As the shear rate is increased the contact time between colliding entities decreases and more fragile aggregates are formed. Shear can also induce aggregate rupture. The rupture mechanism is driven by the applied shear stress counterbalanced by the aggregate cohesion. This mechanism results in the aggregate size reduction. The critical stress for rupture depends on the aggregate size. Larger aggregates are easier to break (Collin and Peuvrel-Disdier, 2005). At low shear rates, aggregation is favored and leads to the formation of large aggregates. As the shear rate is increased, the aggregate size at steady state (after the end of the first crystallisation for a constant solid fraction) is controlled by the dynamic equilibrium between aggregation and rupture. The higher the shear rate is, the smaller the aggregate should be. For high enough shear rates, aggregation should not be possible any more. This simple description of the role of shear on the aggregation process can explain the fact that the magnitude of the viscosity jump decreased as the shear rate increased. This discussion based on the effect of shear on aggregation does not take into account the size and structure of the spherulites constituting the aggregates, which both are influenced by the shear rate as seen in the previous paragraph.

Effect of the shear geometry:

The fact that spherulite size depends on the applied shear rate also means that the structure should be heterogeneous along the radius axis in parallel plate geometries. This heterogeneity of structure in the parallel plate geometries can explain the differences observed on viscosity curves for the same shear rate but obtained with the three geometries. An example is shown in Figure 8 for 10 s^{-1}.

This figure shows that, although the shear history submitted to the palm oil sample was different, the same events occurred: two viscosity jumps followed by viscosity oscillations. The magnitude of the viscosity jump was different with the three geometries. The cone-and-plate geometry gave rise to a uniform structure (except close to the cone centre). The heterogeneous structure generated in the parallel plate geometry led to a lower viscosity. This was enhanced in the 60 mm diameter geometry where the heterogeneous structure had more room to develop.

Zone C: First viscosity plateau

After the sharp viscosity jump due to the first crystallisation, a constant viscosity was recorded for some time while the sample was kept in isothermal conditions at 10 °C and with a constant shear rate. The existence of a viscosity plateau implies that the first crystallisation was finished and that a steady state was reached. At this level, the material was constituted of individual aggregates of solid crystals suspended in a molten medium. As discussed in the previous part, the viscosity jump is related to the aggregate size which is controlled by the applied shear-rate. The lower the shear rate is, the larger the viscosity jump is. The viscosity jump intensity decreases as the shear rate is increased. A

similar tendency was also measured by De Graef et al. (2008) but on smaller solid fat fractions (isotherm at 18°C).

Shear thinning behaviour

Plotting the apparent viscosity versus the applied shear rate shows that the crystalline suspension presents a shear thinning behaviour (as depicted in Figure 9). This behaviour also means a decrease of the apparent solid volume fraction with shear rate increase. The decrease of the apparent solid volume fraction can be due to a simple spatial rearrangement of the same solid fraction under the action of shear as for a simple suspension (Larson, 1999) and/or to a variation of the crystalline fraction under the action of shear. Measurements of the solid fat content by pulsed-NMR in-situ during shear showed that the steady state solid fat content did not vary with the applied shear rate (Mazzanti et al., 2005). A few percent solid fat content decrease with the shear rate increase was determined by the same team (Mazzanti et al., 2008) on a different fat system. The solid fat content decrease was explained by a few degree temperature increase due to the viscous heat generated by the flow of the concentrated suspension at large shear rates.

The main contribution to the shear thinning behaviour of the palm oil crystalline suspension is thus only due to different structural organisations of the same solid fat content resulting from the application of different shear rates. Ng and Oh (1994) measured the solid fat content isothermal conditions and found a 20 % solid fat content after the first crystallisation relative to 48 % solid fat content for the total isotherm crystallisation at 9 °C.

Estimation of solid volume fraction:

The solid volume fraction of the suspension was estimated from the first viscosity plateau using the Krieger–Dougherty equation (Krieger and Dougherty, 1959). This model relates the suspension viscosity (η_{susp}) and the particle volume fraction (ϕ) knowing the maximum random close packing volume fraction (ϕ_{max}) and intrinsic viscosity ([η]) of the system:

$$\eta_{susp} = \eta_m \left(1 - \frac{\phi}{\phi_{max}}\right)^{-[\eta]\phi_{max}}$$

where η_m is the viscosity of the suspending medium (here the viscosity of the liquid palm oil at 10 °C, deduced from the Arrhenius law).

The solid volume fraction ϕ can be evaluated using this equation, η_{susp} and η_m being measured and assuming that ϕ_{max} and [η] are known.

The values of ϕ_{max} and [η] depend on the type, shape and size polydispersity of the particles and give a picture of the structure of the suspension. Since, the application of shear on a suspension results in a more ordered structure, the maximum packing fraction varies with shear (see for example (Larson, 1999)). Originally proposed to describe the suspension in the low shear Newtonian region with the parameters (ϕ_{max0} and $[\eta]_0$), the Krieger-Dougherty equation was found to give good results in the high shear Newtonian region using a specific set of parameters ($\phi_{max\infty}$ and $[\eta]_\infty$). Due to the spherulitic character of the crystals, parameters derived for monodispersed spheres were used to determine the solid volume fraction at low and high shear rates (ϕ_{max0} = 0.64 and $[\eta]_0$ = 2.67, $\phi_{max\infty}$ = 0.68 and $[\eta]_\infty$ = 2.67). Although, Newtonian behaviours were not measured in the low

and high shear regions, the estimation was made for the lowest and highest shear rates. Solid volume fractions were estimated to be around 53 % at 1 s^{-1} and 42 % at 100 s^{-1}. The obtained solid volume fractions are larger the solid fat content determined after the first crystallisation by Ng and Oh (1994) 20 % at 9 °C. This difference between the solid fat content measured by NMR and the solid volume fraction estimated from the viscosity is due to the fact that the second one refers to hydrodynamic space occupancy while the first one measures the real solid phase content. A lower density of the spherulites (more liquid entrapped between the crystallites) and the formation of aggregates (liquid entrapped between the spherulites) lead to a larger apparent solid volume fraction as determined from the viscosity. An example of a second estimation made with the parameters for a random suspension of aggregates of particles gives fully different results (around 30 %, see Table 2). These attempts show that solid volume fraction estimations based on the viscosity magnitude can only be relevant if the parameters of the Krieger Dougherty model (ϕ_{max} and [η]) characterizing the suspension are known, which is not the case. The determination of these parameters would necessitate systematic rheological measurements with different solid fractions (different isotherm temperatures).

Viscosity plateau and pre-shear rate effect

We have seen that the viscosity intensity in steady state is mainly dominated by the aggregation dynamics. The effect of shear on the first crystallisation was also investigated by applying different pre-shear histories. The sample was first submitted to a pre-shear rate during cooling (during the first crystallisation process) followed by a final constant shear rate during the isotherm. The effect of different pre-shear histories was

investigated for different final shear rates. An example of such an experiment is illustrated for a final shear rate of 50 s^{-1} during the isotherm in Figure 10. Experiments were conducted in the 60 mm diameter geometry and this figure illustrates the volume filling artefact encountered with this geometry (all curves should be superimposed in the molten state).

This figure shows that although different pre-shear rates were applied during the crystallisation step, the steady state viscosity intensities at 50 s^{-1} are around the value reached as if the sample was submitted to the same shear rate during the whole experiment. There seems to be an order in the viscosity intensities. But the viscosity order is not correlated to the viscosity difference in the molten state (mentioned just before). The steady state viscosity obtained after a pre-shear rate larger than the final one was higher than the viscosity resulting from a constant shear rate during the whole experiment. This can be related to the structure developed during the pre-shear. If a higher pre-shear rate than the final one was applied, aggregation of entities resulting from the pre-shear was possible and could explain the higher steady state level. In the case of very high shear rates, crystallites should orientate with the flow direction and result in a different crystalline entity (Mazzanti et al., 2003). If the pre-shear was smaller than the final one, the mean aggregate size after pre-shear was larger than the equilibrium aggregate size at the final shear rate and shear could induce some rupture. Shear affects the crystallisation process (crystal size and growth rate evidenced in this study) and the aggregation dynamics. The different pre-shear histories during the crystallisation step result in different aggregate sizes and structures (different size and structure of the spherulites forming the aggregates). The application of a subsequent shear rate modifies

the dynamic equilibrium between aggregation and rupture but cannot erase the primary structure of these aggregates. The viscosity intensity is dominated by the aggregate size (volume fraction effect) which depends on the applied shear rate.

Zone D: The second phase transition

A second viscosity jump was recorded for shear rates from 1 to 300 s^{-1} after the first viscosity plateau leading to a second viscosity plateau (Figure 5). The secondary crystallisation developed during the isotherm (Figures 2) is at the origin of a new aggregation process leading to larger crystalline aggregates which are responsible for the second viscosity jump.

Effect of shear on the secondary crystallisation onset time

Contrary to the first crystallisation, there is a clear impact of the applied shear rate on the onset time of this secondary crystallisation during isotherm condition (directly visible on the viscosity curves, see Figure 5). Figure 11 shows the variation of the onset time with shear rate. This onset time is found to be smaller as the shear rate is increased and to vary linearly with the natural logarithm of the shear rate. Such a dependence was reported by Mazzanti et al. (2005) as a universal shear effect in all phase transitions of fats. In their case, this reduction of onset time is due to an $\alpha \rightarrow \beta'$ phase transition. At low shear rates, aggregates of α nuclei have time to be formed delaying the $\alpha \rightarrow \beta'$ transformation, whereas at larger shear rates, α nuclei remain as individual crystals which can more easily be transformed on β' crystals. This explains the fact that the secondary phase transition appears sooner when the shear rate is increased.

A second viscosity increase was also reported by De Graef et al. (2008). This phenomenon was observed at a different timescale, after 300 min isotherm at 10 s^{-1} (Figure 6 of their paper). The larger isotherm temperature (18°C) may explain the different timescale. The authors attributed this second increase to the (re)formation of a network structure but excluded the possibility of a polymorphism transformation since at that temperature β' crystals were present and are known to be stable.

Zone E: Second viscosity plateau

The secondary crystallisation or phase transition resulted in an enhanced aggregation process and the formation of more compact entities. The aggregation process is consistent with the fact that the viscosity jump magnitude and transient time depend on the applied shear rate. The second viscosity increase was much smaller than the first viscosity increase (first sudden jump). The explanation of the effect of shear on the aggregation process is the same as the one discussed for the first viscosity jump. The steady state size of the aggregates depends on the dynamic equilibrium between aggregation and rupture. The size decreases as the shear rate increases and explains the decrease of the viscosity jump magnitude. This occurs up to a certain shear rate where no more aggregation is possible. Shear rates greater than 300 s^{-1} prevents further aggregation of the system due to the secondary crystallisation process (contact time between colliding entities too small to enable aggregation). The secondary crystallisation may result in more compact entities with no visible viscosity increase.

Zone F: Oscillations

At low shear rates (1-10 s^{-1}) viscosity curves are not smooth at time greater than 1000 s. They show oscillations growing with time and scaling with the rotation period of the rheometer (Figure 5). These oscillations may arise due to the formation of a fat network and subsequent phase rearrangements under shear leading to more compact zones releasing interstitial liquid which resulted in the network rupture. Figure 12 reports averaged shear stress values for the two viscosity plateau zones as a function of applied shear rate. For the second viscosity plateau values, for the lowest shear rates, shear stress did not depend on shear rate which coincides with the zone of oscillations. It means that the material was slipping on the walls of the rheometer, flowing as a solid body. The shear stress evolution at the first viscosity plateau versus shear rate was indicated for comparison. In this case, the shear stress increased with the shear rate over the whole shear rate range.

Oscillations occurred at shear rates lower than about 30 s^{-1}. Under this value, a network structure was formed. Shear rates greater than 30 s^{-1} prevented the network formation.

Conclusion

The present paper describes the effect of shear on the crystallisation process of palm oil. Viscosity measurements were used to determine the structure evolution, in combination with DSC, optical microscopy and small-angle light scattering. While cooling, a first viscosity jump reflects the first crystallisation. The isothermal condition after this first

crystallisation gives rise to a constant viscosity. The structure after the first crystallisation is a suspension of aggregates of spherulites. During isotherm, a secondary crystallisation process is at the origin of a new aggregation process, resulting in the formation of a network at low shear rates.

The effect of shear on the different steps was systematically investigated. Shear was shown to have a strong effect on :

- the first crystallisation step via the spherulite size and growth rate although the crystallisation temperature or the solid fat content (results from Mazzanti et al. (2005)) were not affected by the applied shear rate,
- the steady state structure after the first crystallisation. The structure after the first crystallisation is a suspension of aggregates of spherulites. The structure and size of the aggregates are controlled by the applied shear rate. However the shear-induced structuring of palm oil during crystallisation is not fully reversible since the primary structure of the spherulites is fixed by the applied shear rate and is irreversible.
- the secondary process of crystallisation during isotherm via the onset of this transformation. This process shows characteristic features of a polymorphism transition, with an acceleration of the transition as the shear rates is increased,
- the steady state structure after the secondary crystallisation process. As after the first crystallisation, the steady state structure after the secondary crystallisation is controlled by the applied shear rate.

This study allowed us to determine two characteristic shear rates of crystallised palm oil system after the first crystallisation under shear. 300 s^{-1} appeared to be the critical shear rate above which aggregation is not possible. Even in presence of the secondary crystallisation, aggregation did not proceed. This means that it was the upper limit shear rate for the formation of aggregates under shear. 30 s^{-1} corresponded to the upper limit shear rate for the formation of a fat network under shear. A 3D fat network could form after the secondary crystallisation process for a shear rate lower than 30 s^{-1}, while above this value, the crystallised palm oil formed a suspension of aggregated crystals.

The texture of crystallised vegetal fats and subsequent end products strongly depends on the structure developed during the crystallisation process. This structuring process is strongly influenced by the thermo-mechanical history submitted to the product (cooling rate, degree of undercooling, annealing time, application of a shear flow). This paper shows how the extent of shear affects the different steps of the crystallisation and aggregation processes in the case of palm oil after the first crystallisation.

Acknowledgements

This work was supported by Danone between 2001 and 2003. The authors are grateful to Pierre Aymard for his help and fruitful discussions on this work.

The authors also wish to thank the referees for their useful and interesting comments.

References

Berger KG, Wright WB. 1976. Crystallisation behaviour of palm oil. Paper presented at ISF conference, September 1976, Marseille, France.

Collin V, Peuvrel-Disdier E. 2005. Dispersion mechanisms of carbon black in an elastomer matrix. Elastomery 9, 9-15.

De Graef V, Dewettinck K, Verbeken D, Foubert I. 2006. Rheological behavior of crystallizing palm oil. Eur J Lipid Sci Sci Technol, 108: 864-870.

De Graef V, Goderis B, Van Puyvelde P, Foubert I, Dewettinck K. 2008. Development of a rheological method to characterize palm oil crystallizing under shear. Eur J Lipid Sci, 110: 521-529.

Grigoriev IS, Meilikhov EZ, Radzig AA. 1997. Handbook of physical values. In Grigoriev IS and Meilikhov EZ Editors. CRC Press, Boca Raton.

Haudin JM, Navard P. 1990. Optical studies of polymer organizations. In Fouassier JP and J.F. Rabek Editors. Lasers in polymer science and technology : applications. CRC Press, Boca Raton. Volume IV, p. 33-92.

Jacobsberg B, Ho OC. 1976. Studies in palm oil crystallisation. J Am Oil Chem Soc, 53: 609-617.

Kawamura K. 1979. The DSC therm al analysis of crystallisation behaviour in palm oil. J Am Oil Chem Soc, 56: 753-758.

Kloek W, van Vliet T, Walstra P. 2005. Mechanical properties of fat dispersions prepared in a mechanical crystallizer. J texture studies, 36: 544-568.

Krieger IM, Dougherty TJ. 1959. A mechanism for non-Newtonian flow in suspensions of rigid spheres. Transactions of the Society of Rheology, III: 137-152.

Larson RG. 1999. The structure and rheology of complex fluids. In Gubbins KE Editors. Oxford University Press, New York.

Mazzanti G, Guthrie SE, Marangoni AG, Idziak SH. 2003. Orientation and phase transition of fat crystals under shear. Cryst Growth Des, 3(5): 721-725

Mazzanti G, Marangoni AG, Idziak SHJ. 2005. Modeling phase transitions during the crystallisation of a multicomponent fat under shear. Phys Rev E, 71: 041607-1-3

Mazzanti G, Guthrie SE, Marangoni AG, Idziak SH. 2007. A conceptual model for shear-induced phase behaviour in crystallizing cocoa butter. Cryst Growth Des, 7(7): 1230-1241.

Mazzanti G, Mudge EM, Anom EY. 2008. In situ rheo-NMR measurements of solid fat content. J Am Oil Chem Soc, 85: 405-412.

Ng WL, Oh CH. 1994. A kinetic study on isothermal crystallisation of palm oil by solid fat content measurements. J Am Oil Chem Soc, 71(10): 1135-1139.

Papir YS and Krieger IM. 1970. Rheological studies on dispersions of uniform colloidal spheres-II. Dispersions in nonaqueous media. J Colloid Int Sci, 34, 126-130

Persmark U, Melin KA, Stähl PO. 1976. Palm oil, its polymorphism and solidification properties, Riv Ital Sostanze Gr, LIII: 301-306.

Siew WL, Ng WL. 1995. Partition coefficient of diglycerides in crystallization of palm oil. J Am Oil Chem Soc, 72(5): 591-594.

Siew WL, Ng WL. 1996. Characterisation of crystals in palm olein, J Sci Food Agric, 70: 212-216.

Siew WL, Ng WL. 1999. Influence of diglycerides on crystallisation of palm oil. J Sci Food Agric, 79: 722-726.

Timms RE. 1984. Phase behaviour of fats and their mixtures. Progr Lipid Res, 23: 1-38, 1984

Van Putte KPAM, Bakker BH. 1987. Crystallisation kinetics of palm oil. J Am Oil Chem Soc, 64(8): 1138-1143.

Walstra P, Kloek W, van Vliet T. 2001. Fat crystals networks. In: Sato K, Garti N, Editors. Crystallization processes in fats and lipid systems. New York: Marcel Dekker. p 289-328.

Zhou JZQ, Fang T, Luo G, Uhlherr PHT. 1995. Yield stress and maximum packing fraction of concentrated suspensions. Rheol Acta, 34: 544-561.

Captions for the tables:

Table 1: Growth rate of the spherulitic entities during crystallisation

Table 2: Estimation of the solid volume fraction from the viscosity at the first plateau using the Krieger and Dougherty equation.

Captions for the figures:

Figure 1: DSC thermograms of the cooling of palm oil from 70 °C to -30 °C at different cooling rates: -10, -5 and -0.5 °C/min.

Figure 2: Isothermal heat flow for palm oil sample for 120 min at 10 °C after cooling from 70 to 10 °C without shear. Time zero corresponds to the starting of the isotherm at 10 °C.

Figure 3: Observations by optical microscopy between crossed polarizers of the crystallisation of palm in static and under different shear conditions. Thermal conditions are cooling from 70 to 10°C at -5 °C/min followed by isotherm at 10 °C. Time zero corresponds to the starting of cooling.

Figure 4: Observations of the crystals formed during crystallisation:

a. Spherulites by optical microscopy without shear. Enlargement of picture corresponding to 0 s^{-1}, 607 s, 19.4 °C in figure 3.
b. Spherulites in the same condition as picture a. but observed by small angle light scattering. without shear.
c. Crystals observed in the segregated molten phase after the network destruction under shear.

Observations were performed between crossed polarizers.

Figure 5: Viscosity evolution during cooling -5 °C/min and isotherm at 10 °C under the application of different shear rates in the cone 4° and plate geometry. Zones

corresponding to the different states are indicated (mainly indicated for 1 s^{-1}) and described in the text.

Figure 6: Temperatures of onset of first crystallisation of palm oil during cooling at –5 °C/min. Temperatures obtained for different shear geometries and rates and via different techniques.

Figure 7: a. S.A.L.S. patterns observed during cooling at -5 °C/min and isotherm at 10 °C for the different applied shear rates. All scattering patterns sere recorded in the same conditions. The indication of filter 0.5 means that in order to decrease the scattering intensity an optical filter was introduced on the light path.

b. Evolution of the spherulite radius versus temperature (determined from S.A.L.S. patterns) during cooling at -5 °C/min for different shear rates.

Figure 8: Comparison of the viscosity evolution at a 10 s^{-1} during -5 °C/min cooling and isotherm for the different shear geometries.

Figure 9: Apparent viscosity at the plateau after the first crystallisation of palm oil versus the applied shear rate. Cooling rate –5 °C/min and isotherm at 10 °C. Data were obtained with different shear geometries.

Figure 10: Viscosity measurements of palm oil during cooling at –5 °C/min at different shear rates, then holding at shear rate 50 s^{-1} in the isothermal plateau at 10 °C.

Figure 11: Onset time for secondary crystallisation as a function of shear rate. Time zero corresponds to the starting of isotherm at 10 °C. Data were obtained with different shear geometries.

Figure 12: Shear stress as a function of shear rate for the two viscosity plateau zones. Data were obtained with different shear geometries.

Shear rate (s^{-1})	0	1	10	100-a	100-b
Growth rate (μm/°C)	2.5 - 4	4	4	17	9

100-a denotes the initial measured growth rate.

100-b denotes the mean growth rate.

Table 1

Tarabukina et al.

	Monodispersed sphere assumption (a)			Estimation from data for a certain type of aggregate (b)		
Shear rate (s^{-1})	ϕ_{max}	[η]	Estimated ϕ	ϕ_{max}	[η]	Estimated ϕ
1	0.57	2.67	0.53	0.38	2.4	0.38
100	0.68	2.67	0.42	0.53	4	0.3

a: parameters extracted from Papir and Krieger (1976) for monodispersed polystyrene spheres

b: parameters extracted from Zhou et al. (1995) for silica aggregates (system referred as SWG in their paper).

Table 2

Tarabukina et al.

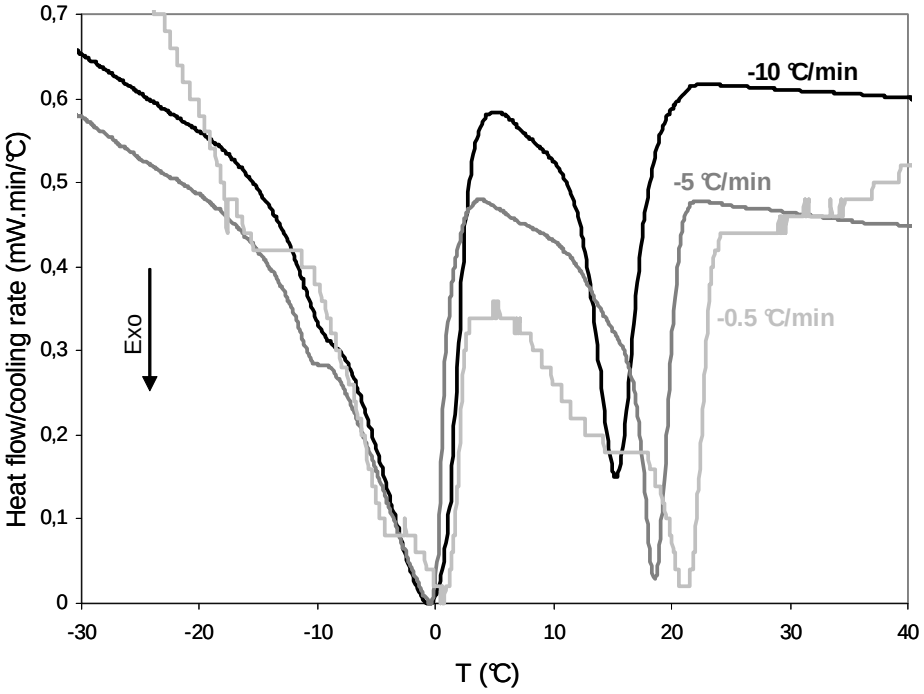

Figure 1
Tarabukina et al.

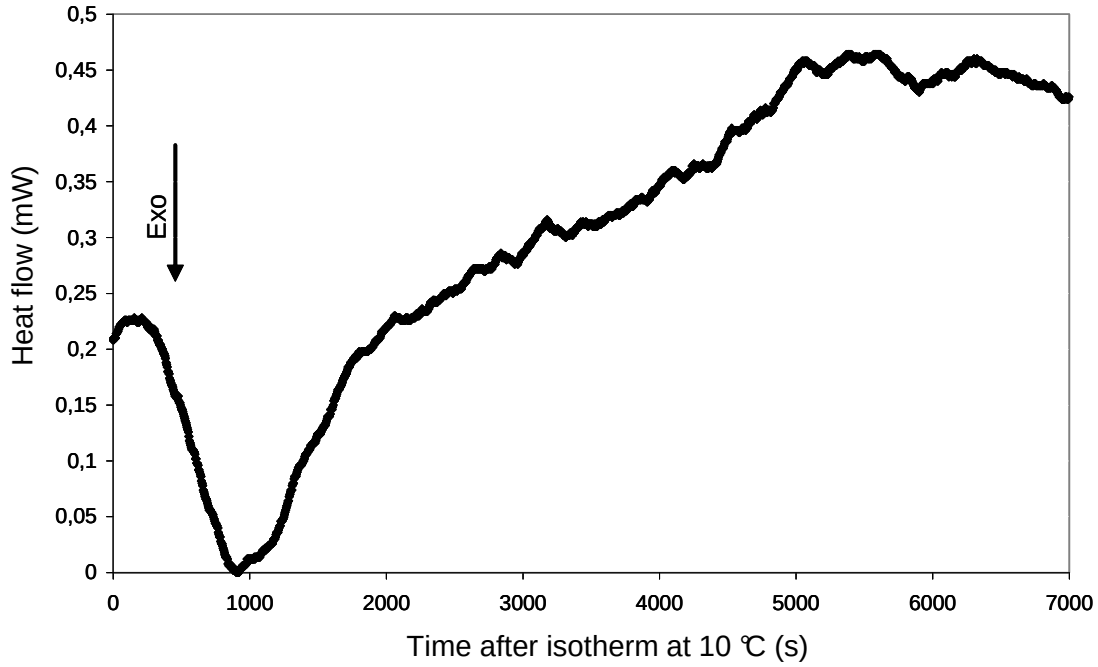

Figure 2
Tarabukina et al.

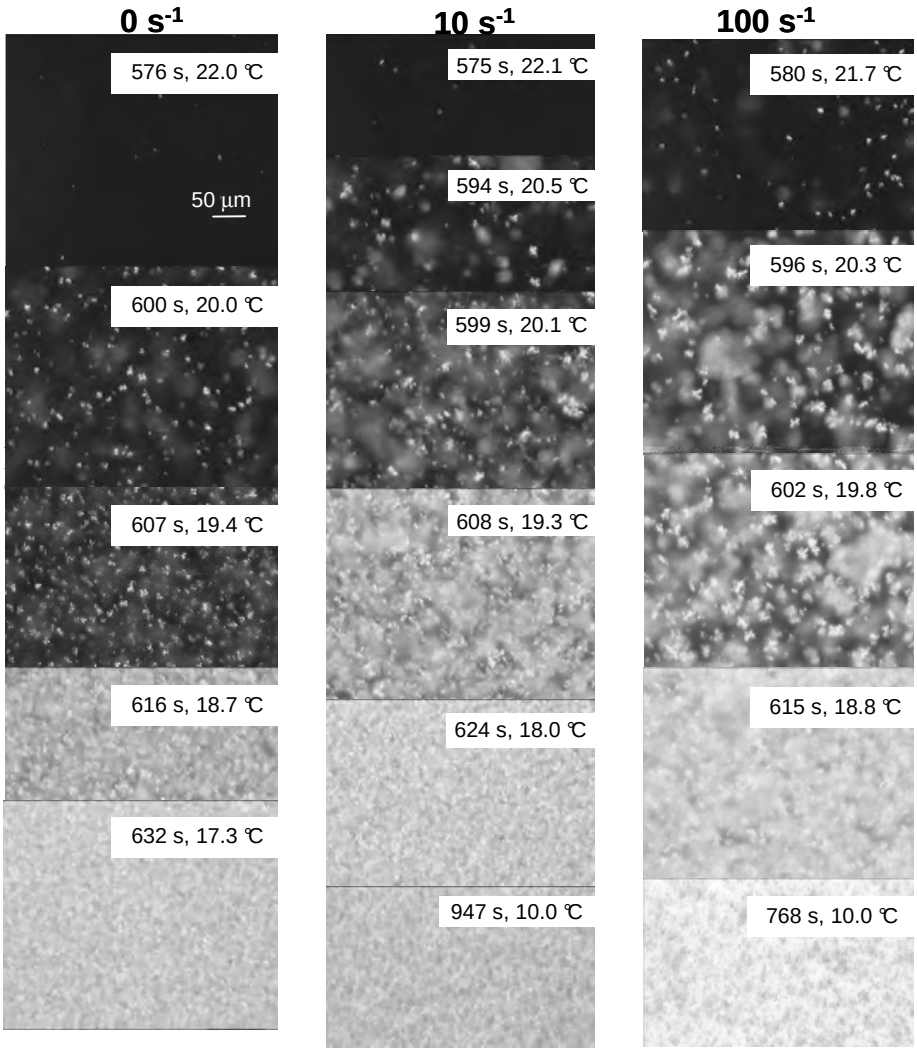

Figure 3
Tarabukina et al.

a

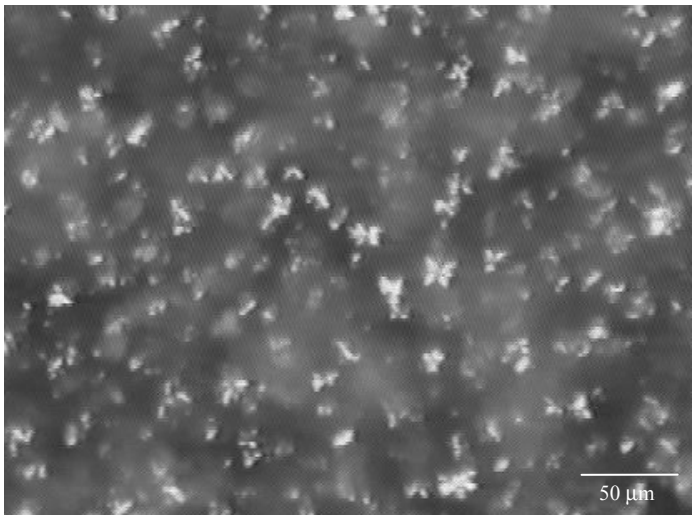

b

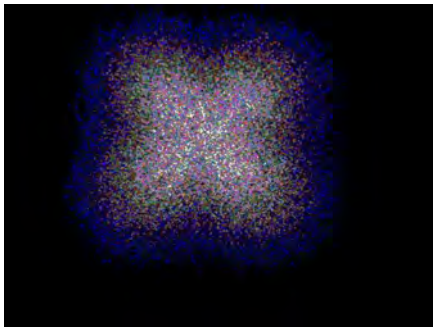

c.

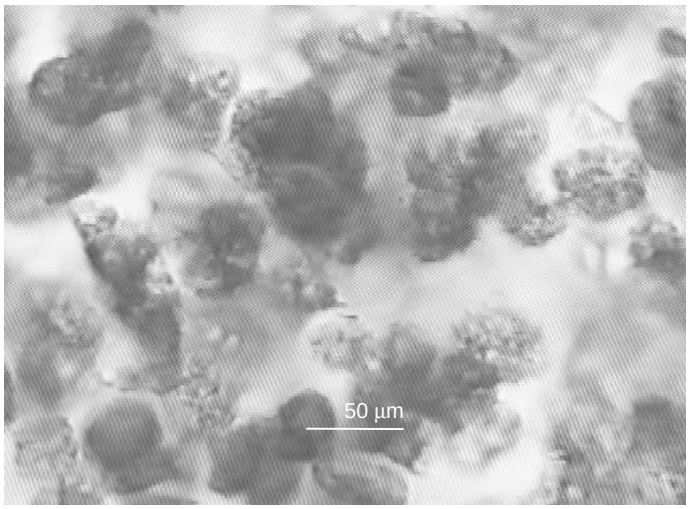

Figure 4
Tarabukina et al.

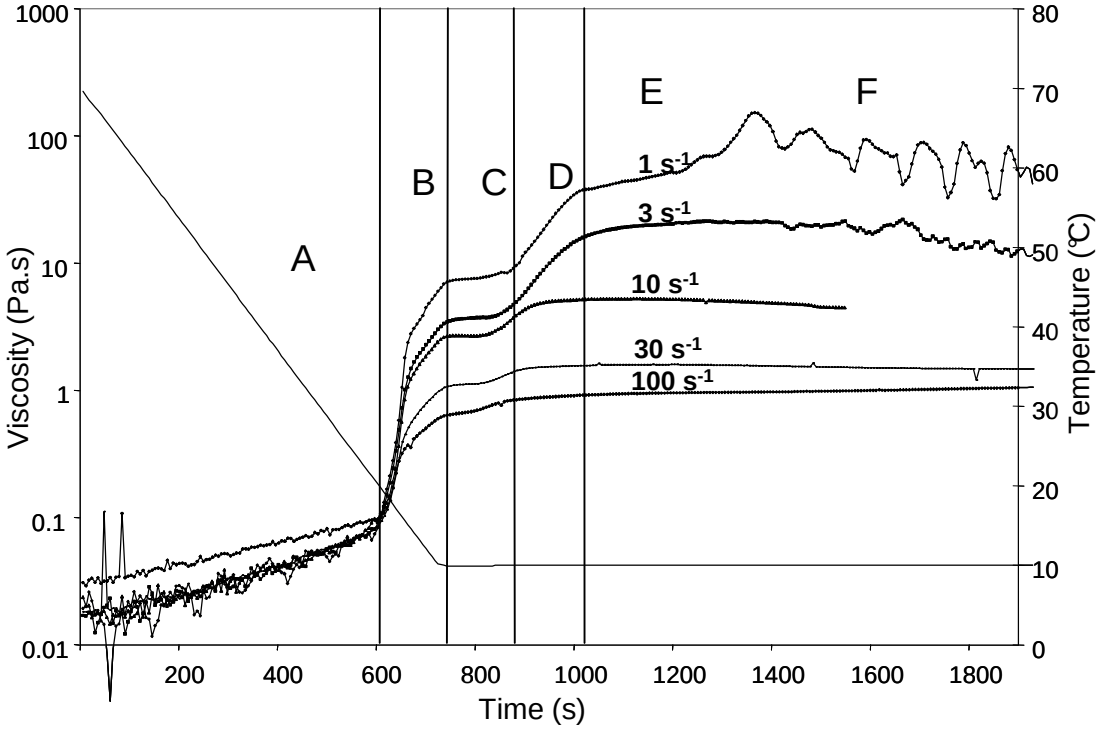

Figure 5
Tarabukina et al.

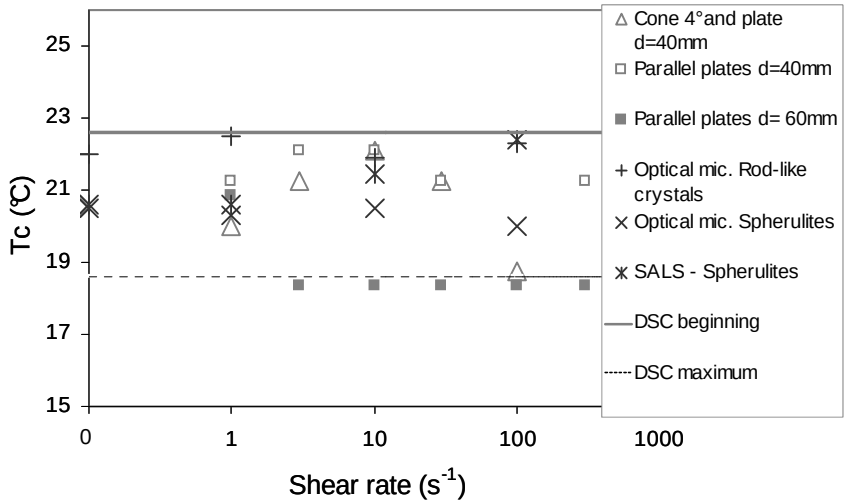

Figure 6
Tarabukina et al.

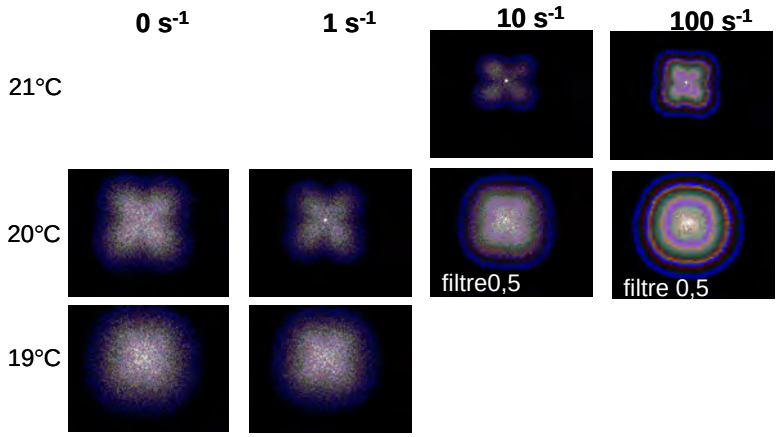

a.

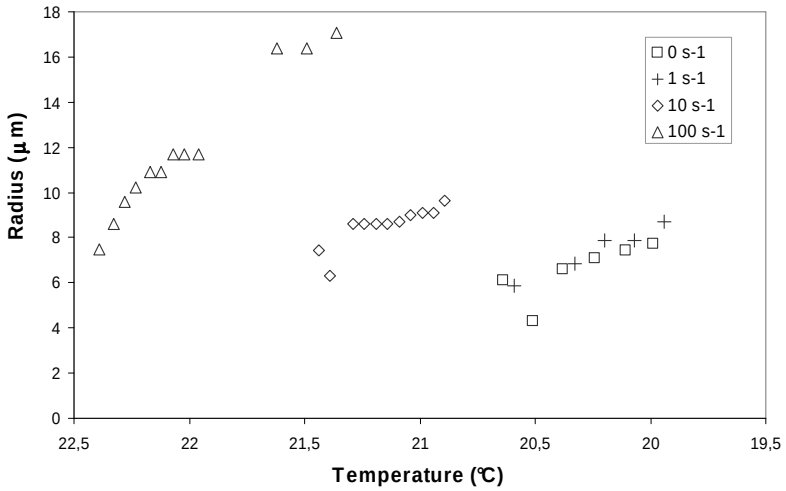

b.

Figure 7
Tarabukina et al.

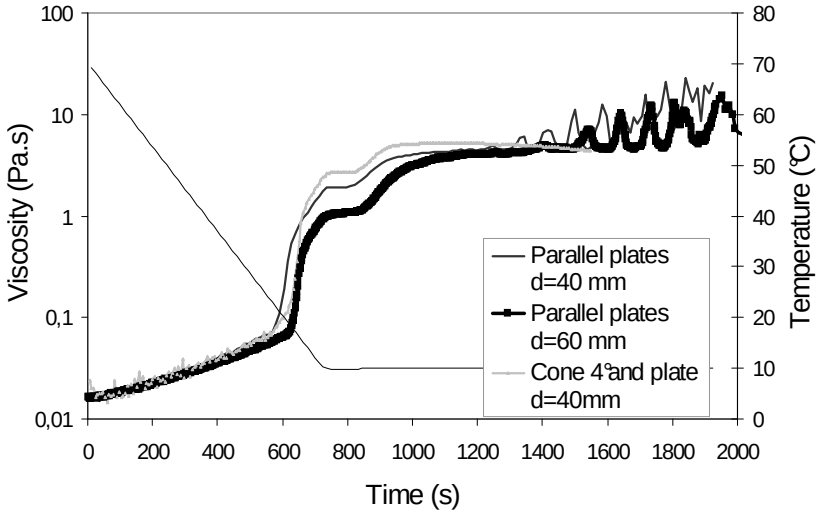

Figure 8
Tarabukina et al.

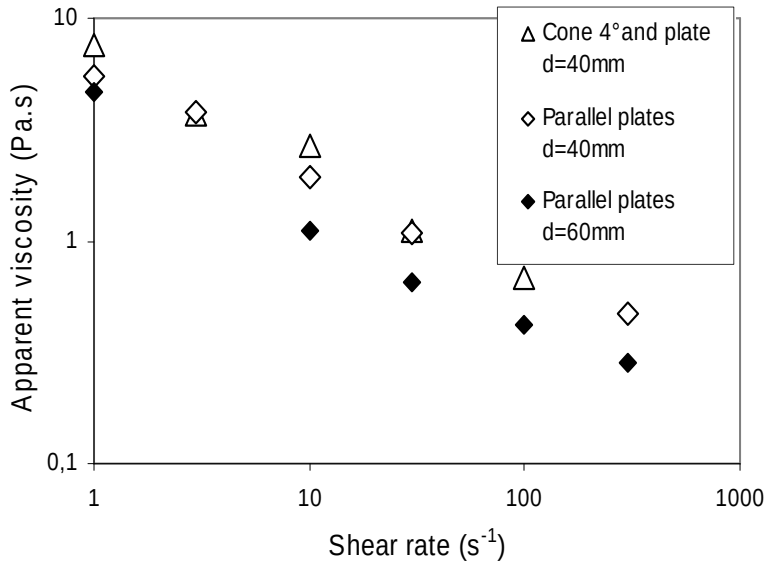

Figure 9
Tarabukina et al.

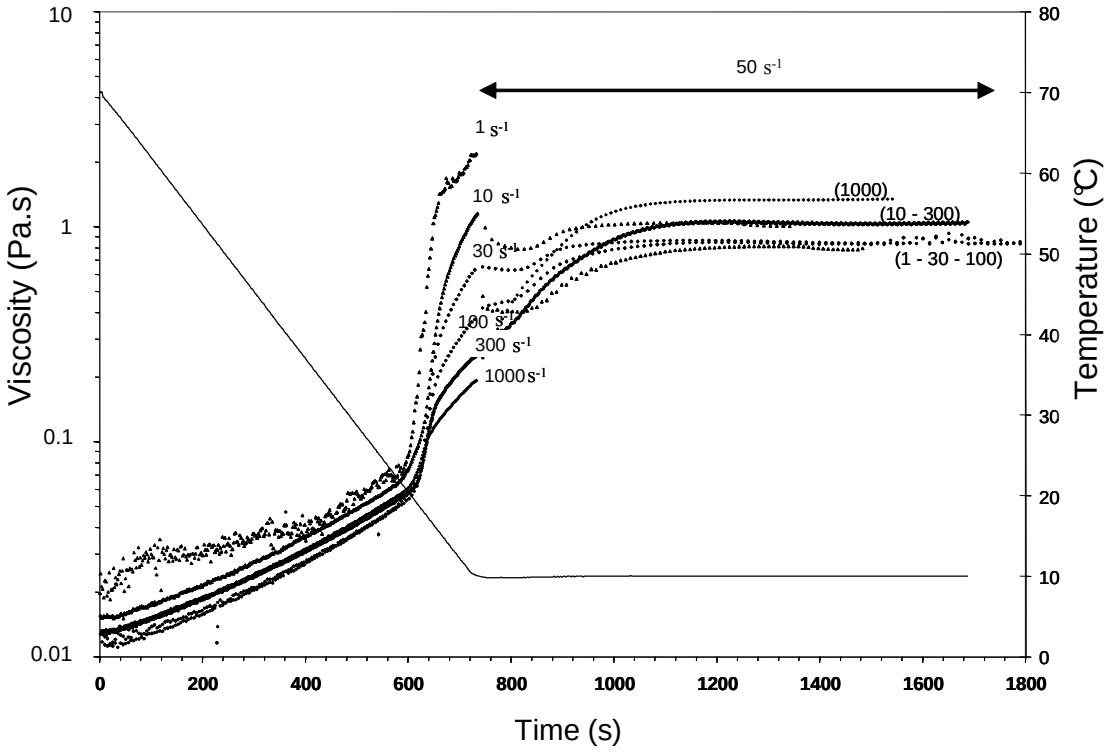

Figure 10
Tarabukina et al.

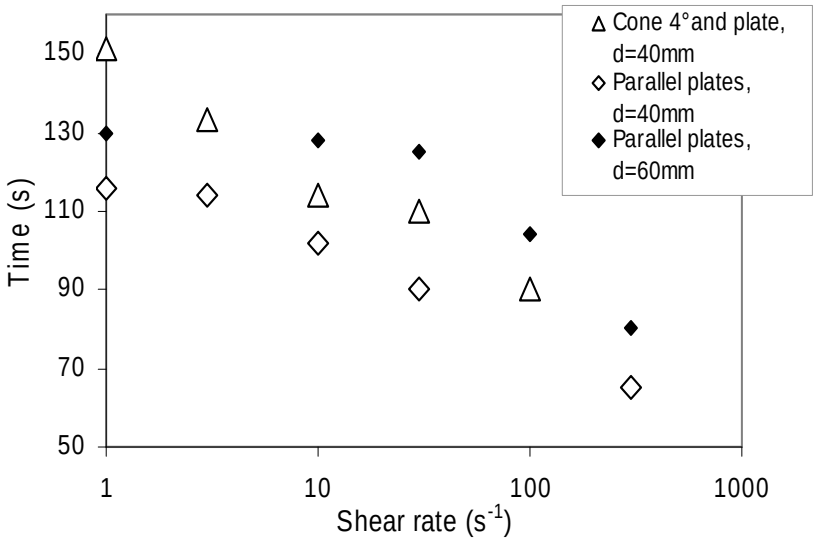

Figure 11
Tarabukina et al.

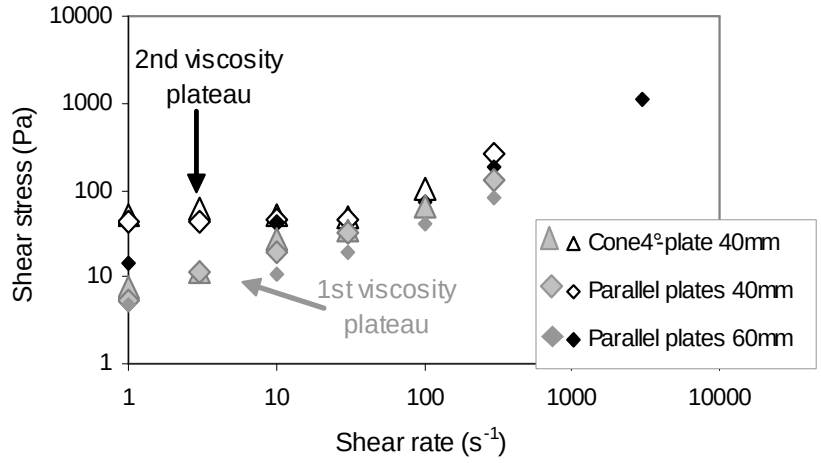

Figure 12
Tarabukina et al.